Relating Binding Affinity to Dynamical Selectivity from Dynamic Monte Carlo Simulations of a Model Calcium Channel

ARTICLE *in* JOURNAL OF PHYSICAL CHEMISTRY LETTERS · JUNE 2010

Impact Factor: 7.46 · DOI: 10.1021/jz100718n

3 AUTHORS, INCLUDING:

Dezso Boda
University of Pannonia, Veszprém
125 PUBLICATIONS **2,839** CITATIONS

THE JOURNAL OF PHYSICAL CHEMISTRY Letters

pubs.acs.org/JPCL

Relating Binding Affinity to Dynamical Selectivity from Dynamic Monte Carlo Simulations of a Model Calcium Channel

Gábor Rutkai, Dezső Boda,* and Tamás Kristóf

Department of Physical Chemistry, University of Pannonia, P.O. Box 158, H-8201 Veszprém, Hungary

ABSTRACT We have performed dynamic Monte Carlo simulations for a model calcium channel and present our results in terms of binding affinity (expressed as the occupancy of the selectivity filter by various ions) and dynamical selectivity (expressed as the flux carried by various ions). We show that the binding affinity of Ca^{2+} versus Na^{+} is always larger than the dynamical selectivity because Ca^{2+} ions are tightly bound to the binding site of the selectivity filter of the channel and, at the same time, their mobility and drift velocity is smaller in this region. We present density and drift velocity profiles of Ca^{2+} and Na^{+} in the channel for various mole fractions of Ca^{2+}.

SECTION Statistical Mechanics, Thermodynamics, Medium Effects

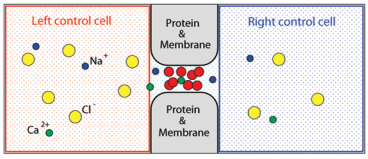

Technological (ion-exchange resins, chromatography) or natural (biological ion channels) devices designed for selective separation of certain components of a mixture work on different time and length scales and also use different molecular mechanisms to distinguish between the different particles. The common feature of these systems is a selective binding of molecules on an adsorbent (macroscopically) or at binding sites (microscopically) and, at the same time, is a transport process in the separation mechanism.

Analogously, the selectivity of these systems can be characterized in two different ways. (1) Binding affinity can be described by the adsorption or binding constants of the various components. This is usually an energetically determined phenomenon. (2) Dynamical selectivity describes which component can penetrate the system in a larger amount in a given amount of time; that is, it describes selectivity on the basis of relative current carried by the various components. This is the primary experimental measurement that is available for ion channels from electrophysiological measurements. These two aspects are sometimes well-separated in macroscopic systems in space and/or time. In systems on the nanoscale or below, however, the two processes occur on the same time and length scale and are intrinsically intertwined.

In an ion-selective channel (through which ions passively flow down their electrochemical gradients), the two kinds of selectivity are clearly defined (1) by the occupancy of the selectivity filter (SF), the major binding site of the channel along the permeation pathway, and (2) by the flux through the channel. The relation of these two properties is the main topic of this Letter.

On a formal level, the diffusion equation establishes a clear connection between them. Integrating the z-component (denoted by (z) in the superscript) of the diffusion equation (for species i) over the $x-y$ dimensions gives

$$J_i^{(z)} \equiv n_i(z)v_i^{(z)}(z) = -D_i(z)n_i(z)\frac{d\mu_i^*(z)}{dz} \qquad (1)$$

where $n_i(z) = \int \rho_i(\mathbf{r})\, dx\, dy$ is the number of ions per unit distance, $\rho_i(\mathbf{r})$ is the density, $D_i(z)$ is the possibly space-dependent diffusion coefficient, $\mu_i^*(z) = \mu_i(z)/kT$ is the chemical potential profile in kT units (k and T being the Boltzmann constant and the temperature), and $v_i^{(z)}(z)$ is the drift velocity profile. The diffusion coefficient and the chemical potential are assumed to be homogeneous in the $x-y$ dimensions. The total flux $J_i^{(z)} = \int j_i^{(z)}(\mathbf{r})\, dx\, dy$ is constant inside of the pore due to conservation of mass ($j_i^{(z)}(\mathbf{r})$ is the z-component of the flux density of species i). In this equation, binding selectivity is formally described by the concentration profile, while dynamical selectivity is formally described by the flux. The diffusion coefficient describes the mobility of ions in the pore. Despite the simple multiplicative relationship between mobility, driving force, and availability of charge carriers, a deeper understanding of the relation between these components on the molecular level is desirable. Binding obviously influences mobility and vice versa. We will use this equation to interpret our results obtained from simulations.

In this work, we use the example of a reduced calcium channel model. It is based on the charge−space competition (CSC) mechanism developed by Nonner et al.[1] that was applied to model the L-type calcium channel,[2−5] the ryanodine receptor (RyR) calcium channel,[6,7] and the sodium

Received Date: May 27, 2010
Accepted Date: June 25, 2010

DOI: 10.1021/jz100718n | J. Phys. Chem. Lett. 2010, 1, 2179–2184

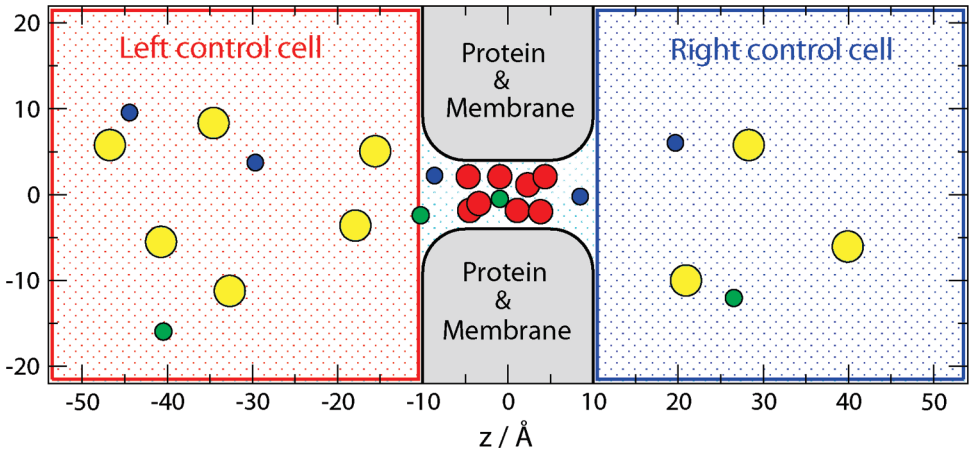

Figure 1. The simulation cell consists of two control cells, where concentrations are controlled by GCMC simulations, and a protein/membrane region that contains the channel. Eight $O^{1/2-}$ ions (red spheres) representing the COO^- groups are confined within the SF ($|z| < 3.6$ Å, $|r| < R - 1.4$ Å, where r is the distance from the axis and $R = 4$ Å is the radius of the SF), but they are mobile otherwise. Green, blue, and yellow spheres represent Ca^{2+}, Na^+, and Cl^- ions, respectively.

channel.[8] Calcium channels are thought to have a highly Ca^{2+}-selective binding site in their SF.[9] The SF of ion channels is the bottleneck for ion flux along their permeation pathway that discriminates between different ions. The SF of the L-type calcium channel, for example, is able to select Ca^{2+} from a bath where Ca^{2+} is present only in a micromolar quantity with a 10 000 fold more abundant monovalent cation in the background.[10,11]

The permeation properties of calcium channels are also unique. In the experiments of Almers and McCleskey[10,11] for the L-type calcium channel, for example, micromolar added $CaCl_2$ reduces the current (compared to no Ca^{2+} present), but the current increases if [$CaCl_2$] is increased above 1 mM. This phenomenon, known as the anomalous mole fraction effect (AMFE), is present in less selective calcium channels too (e.g., RyR), but it is less pronounced.[6,7]

These phenomena are intuitively explained by the highly selective binding site of the calcium channel.[9] At low [$CaCl_2$], a Ca^{2+} ion occupies the SF and prevents Na^+ ions from conducting current. When [$CaCl_2$] is high, an incoming Ca^{2+} ion exerts enough repulsion to knock the Ca^{2+} already occupying the SF out, which is thought to be the basic ("knock off") mechanism of Ca^{2+} conduction through calcium channels.[9,12] In early studies, different binding free energies have been assigned to various binding sites of barriers and wells, and permeation was described with rate theory.

Simulation studies based on well-defined molecular models are desirable for a more thorough understanding of the selectivity and transport mechanisms in calcium channels. Unfortunately, X-ray structures for calcium channels are not available yet. Although more detailed models based on a homology with the known structure of the KcsA potassium channel[13] have been proposed,[12,14−16] only the models based on the CSC mechanism can explain and reproduce experimental results.[4−7]

Simulating the relevant electrolyte concentrations (e.g, micromolar Ca^{2+}) is challenging. Boda et al.[2−5] have used the grand canonical Monte Carlo (GCMC) technique, but because GCMC works in equilibrium, they could not simulate current directly. Therefore, Gillespie and Boda[4] proposed an integrated form of the Nernst−Planck (NP) equation of electrodiffusion in which the density profiles produced by the GCMC simulations are incorporated. In this way, they could calculate the slope conductance of the channel and were able to relate their results to experimental data.[4,5]

Coupling GCMC simulations to the NP equation, however, gives only indirect information about the transport in the calcium channel. In this Letter, we use the dynamical Monte Carlo (DMC) simulation technique[17−19] to simulate current through the model channel of Boda et al.[2−5] directly. We discuss the relation between density and velocity profiles, and we estimate the diffusion coefficient profiles.

Model. The simulation cell is shown in Figure 1. The pore consists of a cylindrical part representing the SF ($|z| < 5$ Å) and two vestibules left and right of the SF ($5 < |z| < 10$ Å). This is the part of the cell for which the DMC simulation were performed. The pore is confined by hard walls that also define the channel protein and the membrane in which it is embedded (for more details, see ref 2).

The baths on the two sides of the membrane are modeled by two rectangular control cells (analogous to the dual control grand canonical molecular dynamics simulation technique[20,21]). The dimensions shown in Figure 1 are typical in our simulations. Because of the large size of the control cells, the strong buffering effect of the SF, and the applied simulation technique (DMC), we did not meet the difficulties discussed by Arya et al.[22] (such as the need for an added streaming velocity). Periodic boundary conditions were applied in the x and y dimensions. In the z dimension, the control cells were externally confined by hard walls, while they were confined by the membrane/protein on the other side. The controll cells and the DMC cell were "open" where they were in contact; that is, ions could move between these cells when MC displacement steps were used.

The ionic concentrations in the control cells were controlled by GCMC simulations where individual ion insertion/deletions were performed. The chemical potentials that correspond to

DOI: 10.1021/jz100718n | J. Phys. Chem. Lett. 2010, 1, 2179–2184

prescribed ionic concentrations were determined using the Adaptive GCMC method of Malasics et al.[23,24]

The SF of calcium channels is a carboxylate-rich site lined by four negatively charged glutamic (E) or aspartic (D) amino acids, similar to the binding sites of calcium-binding proteins (e.g., calmodulin) and chelators (e.g., EDTA, EGTA). The COO^- terminal groups of these amino acids hang into the SF, where they coordinate the passing cations. The model of the SF uses the commonly accepted assumption that these side chains are quite flexible and the carboxylate terminal groups have considerable mobility in the SF. Because of this, we assume that the four COO^- groups are indistinguishable, and therefore, we model them as eight half-charged oxygen ions $O^{1/2-}$ placed in the SF. This model of the COO^- groups has reproduced L-type experimental data,[4,5] and for the RyR calcium channel, it has reproduced hundreds of current−voltage data and predicted AMFEs before they were actually measured.[6,7]

Ions were modeled as charged hard spheres with Pauling diameters (1.9, 1.98, 3.62, and 2.8 Å were used for Na^+, Ca^{2+}, Cl^-, and $O^{1/2-}$, respectively). Water was represented as an implicit solvent with a dielectric constant of $\epsilon = 78.5$ at a temperature of $T = 298.15$ K. Long-range corrections to the screened Coulomb potential were ignored, which did not influence our results.

Dynamic Monte Carlo Method. The DMC method is based on the idea that the sequence of configurations generated by a series of random particle displacements can be interpreted as a dynamical evolution of the system in time.[17−19] DMC reproduces dynamical properties such as the mean-square displacement, although it does not generate deterministic trajectories. DMC does not guarantee an absolute measure of physical time; it only ensures proportionality. Time is expressed as the number of trial MC steps (MCS).

The key parameter of the DMC algorithm is the r_{max} maximum displacement within which a particle is randomly moved with respect to its old position. Our simulations were performed using the algorithm proposed by Rutkai and Kristóf.[19] The main determinant of the r_{max} parameter is the density of the system. In our simulations, this parameter was determined for the whole ion channel, and the resulting value was used for both the high-density SF and the low-density vestibules (the value of r_{max} changed in the range of 0.7−1.8 Å depending on the mole fraction of Ca^{2+}). With this choice, we approximate the fact that the system has high density in the vestibules too because of the presence of water molecules. From this point of view, the DMC technique is more reminiscent of the Brownian dynamics method where dynamical interaction with implicit water is taken into account on the basis of the Langevin equation.

The ratio of currents obtained from DMC simulations for different conditions (e.g., mole fractions) is comparable by design of the used algorithm.[19] This is not necessarily true for the separate, individual currents because they depend on parameters that can change with condition (e.g., system size, r_{max}). Because we used the same system size for every simulation and results are insensitive to small changes in r_{max}, we believe that the Na^+ and Ca^{2+} currents obtained for various mole fractions provide a qualitatively correct picture of the dynamical behavior of the system.

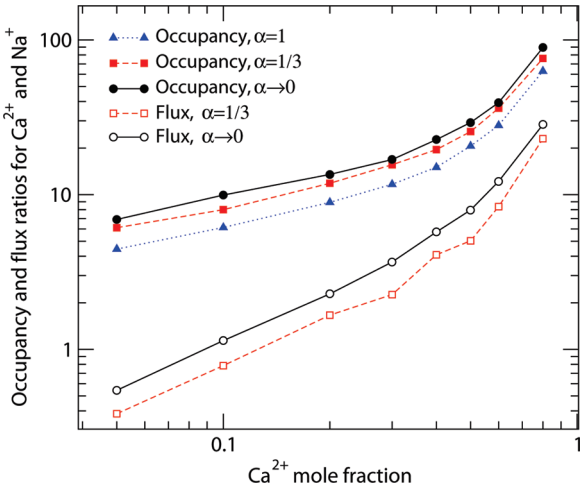

Figure 2. Ratio of the occupancies and fluxes of Ca^{2+} and Na^+ as functions of x_{Ca} for different values of α. Occupancy is defined as the average number of the given ionic species in the SF.

Ionic species were selected for a trial move according to their mole fractions. Time-dependent properties were rescaled with the square root of the particle mass of the given species. The typical length of the simulations was 10^{10} MC moves, including 50 % particle insertions and deletions in the GCMC simulations for the control cells.

In our simulations, the baths (control cells) started right at the entrances of the channel. In reality, there are transition zones of the size of at least a Debye length in these regions with considerable resistances. Because we were primarily interested in the transport mechanisms inside of the channel, we do not consider the role of these zones in this work.

We have performed mole fraction experiments, where the total concentration of the cations (Na^+ and Ca^{2+}) in the left control cell was fixed at 100 mM and the mole fraction of Ca^{2+} (denoted by x_{Ca}) was changed (from now on, mole fraction always means the mole fraction of Ca^{2+}). In the right control cell, we used a smaller total concentration than that on the left-hand side (a chemical potential difference as the driving force of the transport was applied). We always decreased the concentration in the same proportion for Na^+ and Ca^{2+}, namely, $\alpha = c^R(Ca^{2+})/c^L(Ca^{2+}) = c^R(Na^+)/c^L(Na^+)$. For the α parameter, we used 1 (the equilibrium case), 1/3, and 0. The $\alpha \to 0$ case is a limiting case that corresponds to an infinitely dilute electrolyte on the right side that was achieved by using very large negative chemical potentials so that ion insertions were never accepted while ion deletions were always accepted. Formally, this corresponds to an infinitely large driving force. In reality, this never occurs in a steady-state system, but in our simulation, this can be forced by the grand canonical control cells. The equilibrium case ($\alpha = 1$) was performed as a check against GCMC simulations. Excellent agreement was found (data not shown).

The Ca^{2+} versus Na^+ selectivity of the pore can be characterized by the curves shown in Figure 2. The ratio of the occupancies for Ca^{2+} and Na^+ as well as the ratio of the fluxes for Ca^{2+} and Na^+ are plotted as functions of the mole fraction. The main conclusion is that binding selectivity is always larger

DOI: 10.1021/jz100718n | J. Phys. Chem. Lett. 2010, 1, 2179–2184

than dynamical selectivity. For example, for a mole fraction $x_{Ca} = 0.1$, the number of Ca^{2+} is approximately 10 times larger in the channel than the number of Na^+, while the current carried by these two ions is approximately the same.

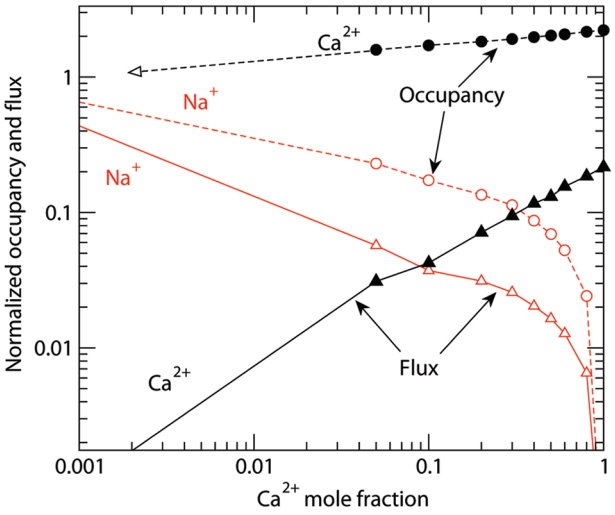

Figure 3. Normalized occupancy (spheres) and flux (triangles) of Ca^{2+} (filled symbols) and Na^+ (open symbols) as functions of x_{Ca} for $\alpha \to 0$. Occupancies are normalized by the Na^+ occupancy in the absence of Ca^{2+}. Fluxes are normalized by the Na^+ flux in the absence of Ca^{2+}.

We can gain further insight by studying the individual currents carried by Na^+ and Ca^{2+}. Figure 3 shows the normalized occupancies and currents of the two cations as functions of mole fraction. Normalization is applied to make a comparison between the two kinds of selectivity more apparent. We show the data for $\alpha \to 0$ because sampling is best for this case (largest driving force); results and conclusions for other values of α are similar.

DMC cannot provide good enough sampling if the mole fraction is too low because it is a rare event that Ca^{2+} diffuses in the vicinity of the channel and enters it. Therefore, we could not simulate mole fractions smaller than 0.05, although the change in the adsorbed number of Na^+ and Ca^{2+} ions takes place in this regime. Equilibrium GCMC simulations indicate that this change occures at about $x_{Ca} \approx 0.001$. A visual extrapolation of the occupancy curves in Figure 3 indicates that this value is probably valid for $\alpha \to 0$ too. Figure 3 shows that at the simulated nonzero mole fractions, there is always significantly more Ca^{2+} in the pore than Na^+ (solid and open circles). At the same time, the mole fraction when the Na^+ flux is the same as the Ca^{2+} flux is about $x_{Ca} \approx 0.1$. Occupancy and flux behave similarly for Na^+ (open symbols), while they behave very differently for Ca^{2+} (filled symbols). It seems that Ca^{2+} likes to be in the pore, but it does not like to pass through it.

Stepping one more layer deeper into the simulation results, we can understand the basic mechanism that is behind this behavior. The first column of Figure 4 shows the axial number

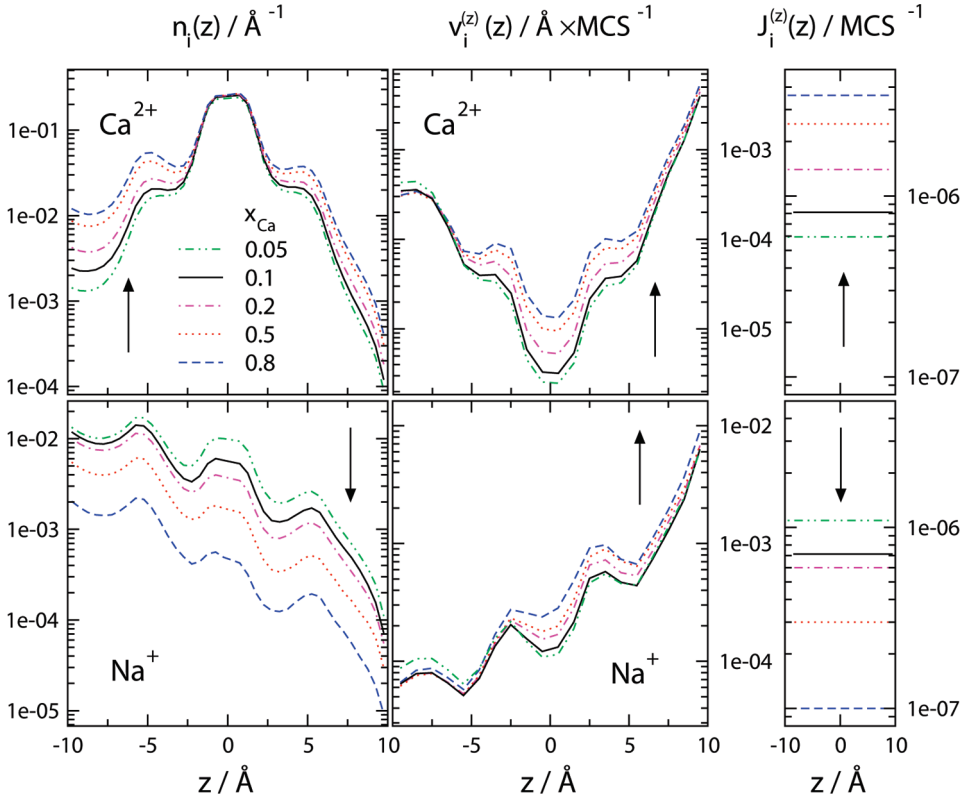

Figure 4. The average number per unit distance $n_i(z)$ (left column), drift velocity $v_i^{(z)}(z)$ (middle column), and flux $J_i(z) = n_i(z)v_i^{(z)}(z)$ (right column) as functions of the axial dimension for various values of x_{Ca}. The top and bottom rows show the curves for Ca^{2+} and Na^+, respectively, ($\alpha \to 0$).

DOI: 10.1021/jz100718n | J. Phys. Chem. Lett. 2010, 1, 2179–2184

density $n_i(z)$ for Ca^{2+} (top row) and Na^+ (bottom row) at different mole fractions. At these mole fractions, there is always a bound Ca^{2+} in the central binding site ($|z| < 2.5$ Å) of the SF. As the mole fraction is increased, the Ca^{2+} density increases outside of this central binding site but does not change inside. Na^+ density profiles, on the other hand, decrease more evenly from left to right, and their magnitude decreases everywhere along the pore axis as the mole fraction increases (the arrows indicate the direction of increasing mole fraction to guide the eye).

The second column shows the drift velocity $v_i^{(z)}(z)$ of Ca^{2+} and Na^+ for the indicated mole fractions. It was calculated as the average distance covered by the ions in the z-direction per MCS. Equation 1 shows that the product of $n_i(z)$ and $v_i^{(z)}(z)$, the flux, must be constant along the z-axis. As the right column shows, this condition is fulfilled. What is more, the flux computed this way is consistent with the results shown in Figure 3, where the flux computed by counting ions crossing the right entrance of the pore is shown (the normalized values are shown in Figure 3). This is a consistency check of the simulations.

The relation of $n_i(z)$ and $v_i^{(z)}(z)$ is apparent in Figure 4 by plotting the ordinate on the logarithmic scale; the sum of the logarithms of these two functions is constant (the curves are mirror images of each other). This means that where a given ion is preferentially accumulated (bound more tightly), it moves more slowly. This is especially interesting for Ca^{2+}. It accumulates in the SF with a large affinity, and therefore, its drift velocity is smaller there. This does not mean that the real thermal velocity of Ca^{2+} ions is smaller. It means that Ca^{2+} ions spend more time in the SF on average.

Figure 4 also reveals different mechanisms behind the change of flux as a function of mole fraction. In the case of Ca^{2+}, the behavior is different in the SF and in the vestibules. In the SF, the flux of Ca^{2+} ions increases with x_{Ca} because the velocity increases, namely, because the ions diffuse faster. In the vestibules, on the other hand, the flux increases because the density of Ca^{2+} ions increases. In the case of Na^+, the latter mechanism dominates; the number of Na^+ ions decreases in the whole pore with increasing x_{Ca}, while their velocity is less influenced.

This result is consistent with the "knock off" mechanism. Conduction of Ca^{2+} ions in the high-affinity SF is a consequence of Ca^{2+} ions entering and leaving the SF more frequently without any change in their number. When more Ca^{2+} is added, the occupancy of Ca^{2+} does not change from its energetically determined value, but Ca^{2+} ions spend less time in the SF due to the repulsive effect of each other.

Equation 1 shows that the drift velocity is proportional to the diffusion coefficient, $v_i^{(z)}(z) = -D_i(z)(d\mu_i^*(z)/dz)$. If we assume that the chemical potential drops linearly in the pore, the derivative of the chemical potential is constant, and the diffusion coefficient is linearly proportional to the drift velocity. In this special case, the $v_i^{(z)}(z)$ profiles in Figure 4 characterize the shape of the $D_i(z)$ profiles too. Then, Ca^{2+} ions are less mobile in the central binding site than elsewhere. Furthermore, the diffusion coefficient of Ca^{2+} is smaller than that of Na^+ by about an order of magnitude. This finding is in agreement with earlier modeling of calcium channels,[4−7] especially with the pivotal work of Nonner and Eisenberg,[26] who first suggested the large difference between Na^+ and Ca^{2+} diffusion coefficients. If the chemical potential drop is not linear, the equation shows that a smaller mobility requires a larger driving force to produce a given drift velocity.

Our analysis shows that the species for which the pore is highly selective has higher occupancy and, at the same time, less mobility in the pore than species for which the channel is not selective. If the pore is narrow enough, this species can block the current of the other(s). Even in wide nanopores, nonlinear behavior (e.g., AMFE) can appear due to the large difference in the transport properties of the various species.[25] Our results are also consistent with the inversion of dynamical selectivity in the OmpF ion channel in the presence of multivalent cations.[27] We propose that this might be a general behavior of pores with high-affinity binding site(s).

AUTHOR INFORMATION

Corresponding Author:

*To whom correspondence should be addressed. E-mail: boda@almos.vein.hu.

ACKNOWLEDGMENT The authors acknowledge the support of the Hungarian National Research Fund (OTKA K75132). We are grateful for the valuable discussions with Dirk Gillespie and Bob Eisenberg.

REFERENCES

(1) Nonner, W.; Catacuzzeno, L.; Eisenberg, B. Binding and Selectivity in L-Type Calcium Channels: A Mean Spherical Approximation. *Biophys. J.* **2000,** *79*, 1976–1992.

(2) Boda, D.; Valiskó, M.; Eisenberg, B.; Nonner, W.; Henderson, D.; Gillespie., D. The Effect of Protein Dielectric Coefficient on the Ionic Selectivity of a Calcium Channel. *J. Chem. Phys.* **2006,** *125*, 034901.

(3) Boda, D.; Valiskó, M.; Eisenberg, B.; Nonner, W.; Henderson, D.; Gillespie, D. Combined Effect of Pore Radius and Protein Dielectric Coefficient on the Selectivity of a Calcium Channel. *Phys. Rev. Lett.* **2007,** *98*, 168102.

(4) Gillespie, D.; Boda., D. The Anomalous Mole Fraction Effect in Calcium Channels: A Measure of Preferential Selectivity. *Biophys. J.* **2008,** *95*, 2658–2672.

(5) Boda, D.; Valiskó, M.; Henderson, D.; Eisenberg, B.; Gillespie, D.; Nonner, W. Ion Selectivity in L-Type Calcium Channels by Electrostatics and Hard-Core Repulsion. *J. Gen. Physiol.* **2009,** *133*, 497–509.

(6) Gillespie, D.; Xu, L.; Wang, Y.; Meissner., G. (De)Constructing the Ryanodine Receptor: Modeling Ion Permeation and Selectivity of the Calcium Release Channel. *J. Phys. Chem. B* **2005,** *109*, 15598–15610.

(7) Gillespie, D. Energetics of Divalent Selectivity in a Calcium Channel: The Ryanodine Receptor Case Study. *Biophys. J.* **2008,** *94*, 1169–1184.

(8) Boda, D.; Nonner, W.; Valiskó, M.; Henderson, D.; Eisenberg, B.; Gillespie, D. Steric Selectivity in Na Channels Arising from Protein Polarization and Mobile Side Chains. *Biophys. J.* **2007,** *93*, 1960–1980.

(9) Sather, W. A.; McCleskey, E. W. Permeation and Selectivity in Calcium Channels. *Annu. Rev. Physiol.* **2003,** *65*, 133–159.

DOI: 10.1021/jz100718n | *J. Phys. Chem. Lett.* **2010,** *1*, 2179–2184

(10) Almers, W.; McCleskey, E. W.; Palade, P. T. Non-Selective Cation Conductance in Frog Muscle Membrane Blocked by Micromolar External Calcium Ions. *J. Physiol.* **1984,** *353*, 565–583.
(11) Almers, W.; McCleskey, E. W. Non-Selective Conductance in Calcium Channels of Frog Muscle: Calcium Selectivity in a Single-File Pore. *J. Physiol.* **1984,** *353*, 585–608.
(12) Cheng, R. C. K.; Tikhonov, D. B.; Zhorov, B. S. Structural Modeling of Calcium Binding in the Selectivity Filter of the L-Type Calcium Channel. *Eur. Biophys. J. Biophys. Lett.* **2010,** *39*, 839–853.
(13) Doyle, D. A.; Cabral, J. M.; Pfuetzner, R. A.; Kuo, A. L.; Gulbis, J. M.; Cohen, S. L.; Chait, B. T.; MacKinnon., R. The Structure of the Potassium Channel: Molecular Basis of K^+ Conduction and Selectivity. *Science* **1998,** *280*, 69–77.
(14) Corry, B.; Allen, T.; Kuyucak, S.; Chung, S.-H. Mechanisms of Permeation and Selectivity in Calcium Channels. *Biophys. J.* **2001,** *80*, 195–214.
(15) Lipkind, G. M.; Fozzard, H. A. Modeling of the Outer Vestibule and Selectivity Filter of the L-Type Ca^{2+} Channel. *Biochem.* **2001,** *40*, 6786–6794.
(16) Barreiro, G.; Guimaraes, C. R. W.; de Alencastro., R. B. A Molecular Dynamics Study of an L-Type Calcium Channel Model. *Protein Eng.* **2002,** *15*, 109–122.
(17) Huitema, H. E. A.; van der Eerden., J. P. Can Monte Carlo Simulation Describe Dynamics? A Test on Lennard-Jones Systems. *J. Chem. Phys.* **1999,** *110*, 3267.
(18) Berthier, L. Revisiting the Slow Dynamics of a Silica Melt Using Monte Carlo Simulations. *Phys. Rev. E* **2007,** *76*, 011507.
(19) Rutkai, G.; Kristóf, T. Dynamic Monte Carlo Simulation in Mixtures. *J. Chem. Phys.* **2010,** *132*, 124101.
(20) Heffelfinger, G. S.; van Swol, F. Diffusion in Lennard-Jones Fluids Using Dual Control Volume Grand Canonical Molecular Dynamics Simulation (DCVGCMD). *J. Chem. Phys.* **1994,** *100*, 7548.
(21) Lísal, M.; Brennan, J. K.; Smith, W. R.; Siperstein, F. R. Dual Control Cell Reaction Ensemble Molecular Dynamics: A Method for Simulations of Reactions and Adsorption in Porous Materials. *J. Chem. Phys.* **2004,** *121*, 4901.
(22) Arya, G.; Chang, H.-C.; Maginn., E. J. A Critical Comparison of Equilibrium, Non-Equilibrium and Boundary-Driven Molecular Dynamics Techniques for Studying Transport in Microporous Materials. *J. Chem. Phys.* **2001,** *115*, 8112.
(23) Malasics, A.; Gillespie, D.; Boda, D. Simulating Prescribed Particle Densities in the Grand Canonical Ensemble Using Iterative Algorithms. *J. Chem. Phys.* **2008,** *128*, 124102.
(24) Malasics, A.; Boda, D. An Efficient Iterative Grand Canonical Monte Carlo Algorithm to Determine Individual Ionic Chemical Potentials in Electrolytes. *J. Chem. Phys.* **2010**, *132*, 244103.
(25) Gillespie, D.; Boda, D.; He, Y.; Apel, P.; Siwy, Z. S. Synthetic Nanopores As a Test Case for Ion Channel Theories: The Anomalous Mole Fraction Effect without Single Filing. *Biophys. J.* **2008,** *95*, 609–619.
(26) Nonner, W.; Eisenberg, B. Ion Permeation and Glutamate Residues Linked by Poisson−Nernst−Planck Theory in L-Type Calcium Channels. *Biophys. J.* **1998,** *75*, 1287–1305.
(27) M. Aguilella-Arzo, Calero, C.; Faraudo, J. Ionic Correlations at the Nanoscale: Inversion of Selectivity in a Bio-Nanochannel. See: http://arxiv.org/abs/1005.0278v2.

DOI: 10.1021/jz100718n | *J. Phys. Chem. Lett.* **2010,** *1*, 2179–2184